ABSOLUTE DATING OF AEOLIAN SEDIMENTS IN RELATIONSHIP TO THE DEVELOPMENT OF THE CITY OF GHENT: FIRST RESULTS

Jasper Van Nieuland[1,*], Dimitri Vandenberghe[1], Frank Gelaude[2], Peter Van den Haute[1]

[1]*Laboratory of Mineralogy and Petrology (Luminescence Research Group), Department of Geology and Soil Science, Ghent University, Krijgslaan 281 (S8), B-9000 Ghent, Belgium*

[2]*Conservation of Monuments and Landscapes, Antwerp University, Belgium*

ABSTRACT

Today's physical landscape in the Ghent city area (E Flanders, Belgium) is the result of human activity. Previous studies that aimed at understanding the city in its former environmental context focused on reconstructing the hydrographical network. The role of Late Quaternary aeolian processes and landforms has not been considered. Incited by a reappraisal of the evidence in historical records, our study aims at contributing to an improved understanding of the significance of this windblown (micro) relief.

In this paper, we report on results from optical dating of two aeolian sequences (near the "Emile Braunplein" and the "Hoogpoort") in the historical city centre. Optical dates of ~ 11 ka – ~ 15 ka indicate deposition during the Late Glacial, and allow refining the Quaternary geological map of the area. Anthropogenic activity on this sediment is supported by a cart mark observed in the upper part of the sediments and post-sedimentary reworking of the top of the "Hoogpoort" sequence. This confirms that Pleistocene aeolian formed elevations were present and at least as relevant to Ghent city's settlement history as a local Tertiary outlier (the "Blandijnberg") and the regional riverine environment.

1. INTRODUCTION

The city of Ghent (East Flanders, Belgium) is situated in the confluence region of the rivers Scheldt and Lys (Fig. 1a). The environment consisted of many branched streams crossing wetlands that were periodically inundated. Near this cross point of waterways and landroads a "*portus*" arose, a place where traders and merchants lived and became rich. Due to this location and the commercial rights Ghent grew from distinct habitation nuclei (Fig. 1b) to one of the largest and most important cities in northern Europe during the Middle Ages (Capiteyn et al., 2007). The development and expansion of the city implied that its inhabitants had to alter the natural hydrographic system. Many human interventions have indeed been described: rivers were straightened, weirs and bridges built, dikes and reinforcements thrown up along riverbanks (Gelaude, 2010b). Previous studies that aimed at understanding the city's settlement history in relation to the former landscape reflect a pronounced focus on this interaction between man and its fluvial environment. Although they were likely the favourable locations for settling, given

the wet and marshy environment, the role of local elevations (such as small hills and ridges) has received minor attention. The only hill that is thought to have influenced the city's setting and history is a Tertiary outlier locally known as the "Blandijnberg" (Tavernier, 1954). Although an old abbey ("Saint Pieter") was founded on that hill, both the historical city centre *portus* and one of Ghent's oldest abbeys ("Saint Bavo") were established around it. The importance of the surrounding area of the "Blandijnberg" to the history of Ghent is partly revealed by historical city maps on which small hills are depicted in and outside the city walls. However, so far, nearly no attention has been paid to these hills, but the mills on top of them reveal a major importance for economic activities. Dumont (1951) describes them briefly in an urban context as being "present and preserved in the relief of the city although they were levelled due to the construction of streets. Their relative height today is smaller than before. Their names and location is preserved in the toponymy". Further detailed descriptions are absent in the historical record.
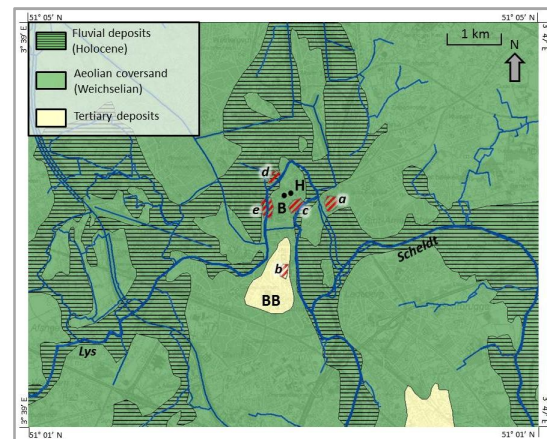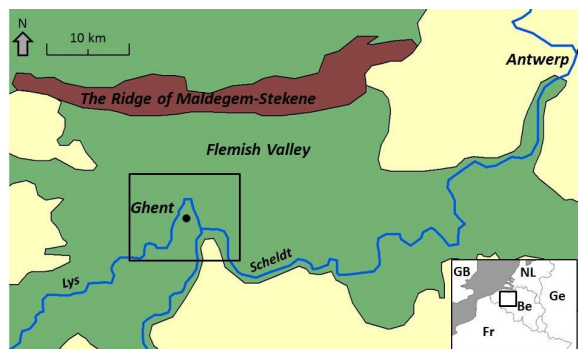
Figure 1: a: Position of the Maldegem-Stekene coversand ridge within the Flemish Valley (Pleistocene deposits; redrawn form De Moor, 1981); b: Simplified geological map of the Ghent city area (Vermeire et al., 1999); it illustrates the complex interaction between aeolian and fluvial processes during the Young Quaternary in the area. Outside the Flemish Valley area and the Blandijnberg (BB), the substrate mainly consists of a thin reworked Pleistocene coversand layer that is underlain by Tertiary sediments. The Flemish Valley essentially consists of Pleistocene (Weichselian sands on top) aeolian sediments in which the Holocene drainage system incised, resulting in fluvial deposits. The early settlement nuclei are also indicated, (a): Saint-Bavo Abbey, (b): Saint-Pieters Abbey, (c): Scheldt-Portus, (d) Oudburg-Gravensteen, (e): Lys-Portus, as well as the two sample locations (B: Emile Braunplein; H: Hoogpoort). From the toponymic research of Gysseling (1954), we could extract over 50 toponyms, indicating that the area of Ghent must have been dotted very densely by dunes. This is also corroborated by historical maps such as those by Braun and Hogenberg (1572; Fig. 2a) and Horenbault (1619; Fig. 2b) which show different districts in the city of Ghent occupied by numerous small hills. The difference between the historical and the present landscape merely illustrates the impact of urban development on the landscape (Gelaude, 2010a).

a)

b)

Figure 2: Maps showing two districts of the city of Ghent in the 16-17th century (adopted from Capiteyn, 2010). They are cutouts from the historical maps of (a) Braun and Hogenberg (1575) and (b) Horenbault (1619). Note that numerous hills are depicted near the city centre; their position next to rivers suggests that they are river dunes

In this paper, we report on quartz-based optical dating of two sequences in the historical centre of Ghent, which were identified through our reappraisal of the historic maps and toponyms. The study frames in a larger project that aims at refining our understanding of the environmental variables that governed the development of the city, with a particular emphasis on the aeolian context.

2. GEOARCHAEOLOGICAL SETTING

Ghent is located in the Flemish Valley, a large North-South palaeovalley that has alternately been filled (mainly aeolian) and eroded (mainly fluvial) and reworked during the Upper Pleistocene. This drainage system is thought to have been dammed by the formation of an aeolian sand ridge during the Weichselian Pleniglacial and the Late Glacial (De Moor, 1981). This sand ridge, locally known as the Maldegem-Stekene coversand ridge (Fig. 1a), forced the rivers to change their direction from North to East. During the Late Glacial, river behaviour also changed from braided to meandering (De Moor, 1981). Exactly on the place where the change in river direction occurred, Ghent developed in an area with a complex (palaeo-) hydrographical network from which the riverbanks and marchlands are a last time overlain during the Holocene by fluvial sediments. As such, the city of Ghent started as one or more distinct settlements in a coversand area using the marsh and wetlands, incised by many branched streams and gullies. In this environment, elevated areas

were to be preferred for habitation. At present, the most pronounced elevation in the Ghent city area is a geological outlier (up to 20 m above the surrounding area), locally known as the "Blandijnberg". It is underlain by marine clays of Eocene age that were able to withstand erosion of a large Flemish (palaeo)valley during the Quaternary (Vermeire et al., 1999; Fig. 1b).

The chronostratigraphic position of coversands is, due to their omnipresence in the field and the intercalation of peat layers and organic soils, been subjected to many dating studies (Kasse, 1999; 2002; Koster, 1988). This is in contrast to the age control of dunes, of which the position is poorly known and still debated (Bogemans and Vandenberghe, 2011). Because studies on the substrate of the city of Ghent are scarce (e.g. Tavernier, 1936), a short overview on studies on this material in the broader area of the Flemish Valley is outlined in order to interpret and discuss the results, assuming the natural environment of the Ghent city area may be considered as analogous.

De Moor (1981) distinguishes dunes from sand ridges from a morphological point of view. The latter result from the accumulation of sediments during the Late-Pleniglacial or Late Glacial derived from a large source area and occur as parallel ridges perpendicular to dominating winds. Although this assumes that sand ridge formation activity is related to colder and dryer periods, consensus on the timing of the depositional phases is far from reached mainly because the known theories are based on indirect dating methods. Furthermore, grain size distributions

prove on a usually smaller grain size for cover-sands ridges (Kasse, 2002).

Dunes, on the other hand, are smaller land-forms; they are composed of coarser sediments (≈ 200 μm) and originate from local source areas. Their position and occurrence in the field is scattered. Many different causes and timings of dune formation have been published as local areas can dry up very fast by, for example, a dryer period (e.g. the Younger Dryas; Verbruggen et al., 1991; Bogemans and Vandenberghe, 2011), the incision of rivers during the Boreal (De Moor, 1981), and deforestation in the Subatlanticum (Castel et al., 1989; Derese et al., 2010a). Because of their specific morphography, the toponym 'berg' is often used (Gysseling, 1954).

3. OPTICAL DATING

Optically Stimulated Luminescence (OSL) dating provides the only means to obtain direct age information for the deposits. Over the past few years, it has been applied successfully to comparable deposits in this area (Derese et al., 2010a, 2010b; Bogemans and Vandenberghe, 2011).

3.1 Sample locations and field observations

At two localities in the historical city centre ("Emile Braunplein" and "Hoogpoort"), infrastructural works allowed us to investigate and sample the sedimentary record. Both sites are located on the "Zandberg" area, which is an elevation holding almost the entire historical city centre of Ghent and is located close to the "Blandijnberg". The Hoogpoort is situated at 12.95 m above sea level, and the "Emile Braunplein" at 10.94 m.

The sequences consist of pale, non-laminated quartz rich sands overlain by the archaeological ("black") layer. No discordances, such as pavements, peat or soils, or cross bedding are observed. The analysed sequences vary between 0.6 m and 1 m and are located on an aeolian formed ridge, as shown in Fig. 1b. In the top of the aeolian deposits, a refilled cart mark is observed in the "Hoogpoort" sequence.

### 3.2 Sampling, sample preparation and analytical facilities

At both localities, the sediments were sampled at closely spaced vertical intervals of ~20 cm. The samples were collected by hammering stainless steel cylinders into freshly cleaned sediment exposures. Eight OSL samples were taken in total, three at the "Emile Braunplein" sequence (GLL-102501 to -3) and five at the "Hoogpoort" sequence (GLL-102504 to -8). About 1 kg of the surrounding sediment of each sample was collected for dose rate determination. For each sediment unit, at least one undisturbed sample was collected for evaluating the time-averaged moisture content.

Sand-sized quartz grains were extracted from the inner part of the sampling tubes using standard techniques (HCl, H_2O_2, wet and dry sieving, HF). For both sequences, we have used grains from the 125-180 μm fraction for analysis although it is noted that the sediment texture of the samples from the "Emile Braunplein" is generally finer (Fig. 3). The purity of the quartz extracts was confirmed by the absence of a significant infrared stimulated luminescence (IRSL) response at 60°C to a regenerative beta dose. Sensitivity to IR stimulation was defined as significant if the resulting signal amounted to more than 10% of the corresponding OSL signal (Vandenberghe, 2004) or if the IR depletion ratio deviated more than 10% from unity (Duller, 2003). For measurement, quartz grains were mounted on stainless steel discs using silicon oil as adhesive. All luminescence measurements were made with an automated Risø TL/OSL/DA-12 reader equipped with blue (470 ± 30 nm) LEDs and IR laser diode (830 nm); the luminescence signals were detected through a 7.5 mm thick Hoya U-340 UV filter. Details on the measurement equipment can be found in Bøtter-Jensen et al. (2003).

Equivalent dose determination was carried out using a single-aliquot regenerative-dose (SAR) protocol (Murray and Wintle, 2000). Optical stimulation with the blue diodes was for 40 s at 125°C.

We adopted a preheat of 10 s at 240° C prior to measurement of the natural and regenerated signals, while the response to the test dose was measured following a cutheat to 160°C. After each measurement of the test-dose signal, a high-temperature cleanout was performed for 40 s at 280°C (Murray and Wintle, 2003).

a)

Emile Braunplein (GLL-102502)

b)

Hoogpoort (GLL-102506)
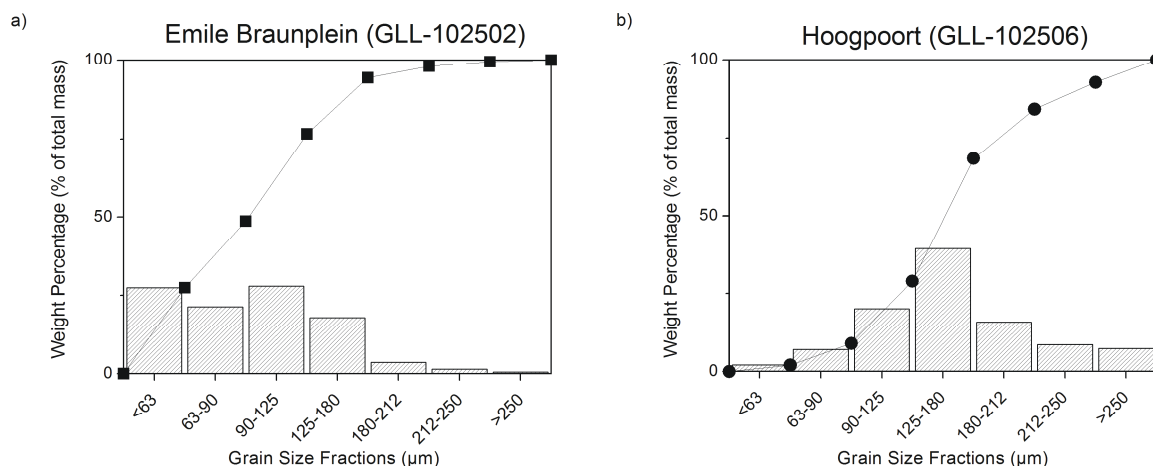
Figure 3: Grain size distributions for a representative sample for the "Emile Braunplein" (a; GLL-102502) and the "Hoogpoort" (b; GLL-102506). The data were obtained through dry sieving during OSL sample preparation. For each sample, the weight of each fraction is plotted in a histogram while the cumulative percentage is plotted in a curve.

It has been shown (Cunningham and Wallinga, 2010) that the net signal is most dominated by the fast component when it is calculated from the initial part of the OSL decay curve, minus a background evaluated from an immediately following interval (rather than from the end of the stimulation period).

Comparison of results obtained using "early" and "late" background subtraction thus offers a means to test for the significance of slower components; all calculations were made twice, by using the initial 0.32 s of the decay curve minus a background evaluated from both the 0.32-1.12 s (early background) and 36.16–40 s interval (late background).

Determination of the dose rate was based on low-level high-resolution gamma-ray spectrometry. The sediment was dried at 110°C until constant weight, pulverised and homogenised. About 140 g of material was then cast in wax (see e.g. De Corte et al., 2006) and stored for at least one month before being measured on top of the detector; each sample was counted for at least 2 days.

3.3 Luminescence characteristics and equivalent doses

A representative OSL decay and SAR dose-response curve for an aliquot of sample GLL-102505 are shown in Fig. 4. The OSL signal decays fast with stimulation time, suggesting that is dominated by the fast component. The growth curve can be represented well by a single satura-

tion exponential function; the recycling ratios are indistinguishable from unity and recuperation is less than 1 % of the sensitivity corrected natural OSL signal. A dose recovery test (Murray and Wintle, 2003) was performed to evaluate the suitability of the SAR procedure. In this test, 6 natural aliquots of each sample were bleached twice for 250 s using blue diodes at room temperature; the two bleaching treatments were separated by a 10 ks pause.

$D_e = 13.3 \pm 1.3$ Gy
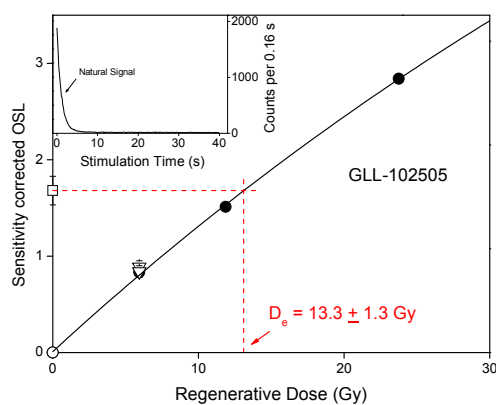
Figure 4: Illustrative growth and OSL decay curve (inset) for an aliquot of 125-180 μm quartz grains extracted from sample GLL-102505. The solid line is the fit of the data to a single saturating exponential function. The open triangle represents a repeat measurement of the response to the first regenerative dose (recycling point). The equivalent dose (D_e) is obtained by interpolation of the sensitivity-corrected natural OSL signal (open square) on the corrected growth curve. The response to a zero regenerative dose is indicated by the open circle (recuperation).

The aliquots were then given a known laboratory dose equal to the estimated equivalent dose, and subsequently measured using the SAR-protocol. Within analytical uncertainty, most ratios of recovered to measured dose do not differ by more than 5% from unity; the overall ratio ± 1 standard error (n = 48) is 1.02 ± 0.02 using the early and 0.98 ± 0.01 using the late background.

The overall average recycling ratios are 0.99 ± 0.01 and 0.98 ± 0.01, while the overall average recuperation amounts to 0.09 ± 0.04% and 0.40 ± 0.05%, respectively. The negligibly small differences illustrate the signals are dominated by the fast component.

For each sample, 15 replicate measurements of the equivalent dose (D_e) were made using large (8mm diameter) aliquots. Values were accepted if, for both early and late background subtraction, recuperation remained below 5% of the corrected natural OSL signal, the recycling ratio, OSL IR depletion ratio and IRSL/OSL ratio did not exceed a threshold set at 10%, and the D_e was within three standard deviations of the mean.

The overall average ratio between the D_es obtained using early and late background is 1.01 ± 0.01 (n = 117), implying that the choice of the integration intervals does not affect the age determination significantly.

For age calculation, we have therefore retained late background subtraction. This approach yields the most precise values of D_e, while still being derived from an OSL signal that is dominated by the fast component, and passes all procedural tests. The average values (± 1 standard error) are summarized in Table 1.

3.4 Dose distributions

For sample GLL-102504, the distribution of equivalent doses (Fig. 5a) was investigated using small (2 mm diameter) aliquots.

Considering the location of the sediments close to an anthropogenic (palaeo-surface), the main purpose was to investigate whether they are likely to be affected by post-depositional processes. A dose recovery distribution (Fig. 5b) was also carried out to distinguish the effects of measurement and instrumental uncertainties from external sources of scatter (see e.g. Vandenberghe et al., 2009).
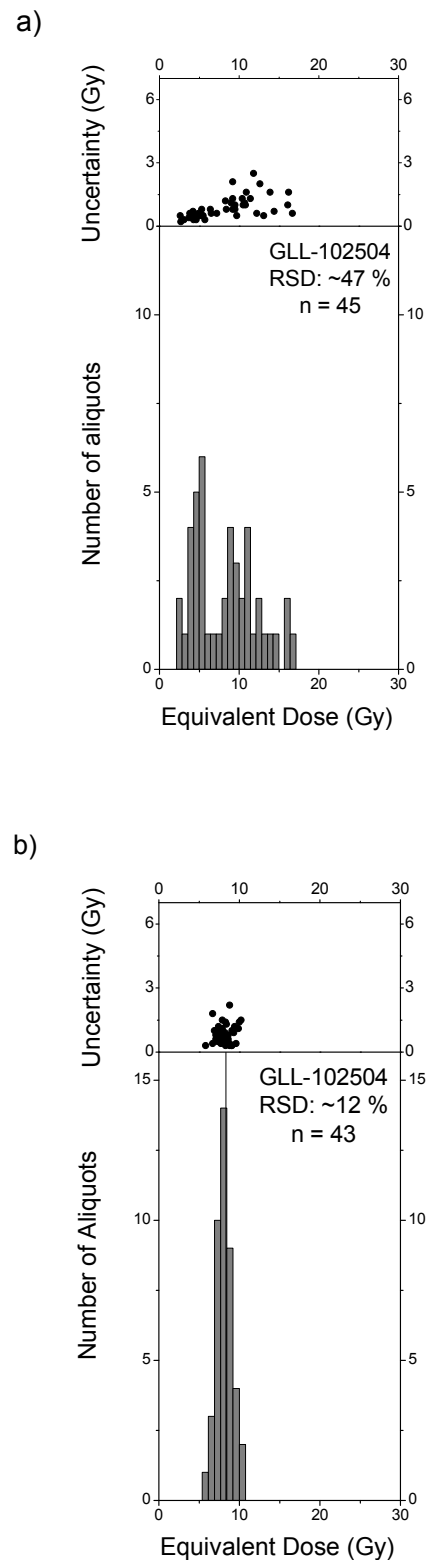
Figure 5: Results for small-aliquot analyses for sample GLL-102504: (a) D_e distribution, and (b) dose recovery data; the given dose is indicated in the histogram by a vertical line. A plot of D_e versus uncertainty is shown above each histogram; the median from this uncertainty distribution was used for binning the data.

Homogenous bleached, non-reworked sediments approach narrow and symmetrical histograms. Asymmetric, broad distributions, on the other hand, can be explained by either a difficult to bleach transport process, such as some colluvial processes (Fuchs and Lang, 2009), or post-depositional reworking (Vandenberghe et al., 2009).

Despite on the flanks of the steep "Blandijnberg" outlier (Tavernier, 1936), no significant slope processes are described in this area. Thus, the broad palaeodose distribution of GLL-102504 (RSD ~ 47%) is mainly attributed to post-sedimentary reworking due to bioturbation or human.

3.5 Dosimetry

The dosimetric information is summarised in Table 1. Radionuclide activity concentrations were converted to dose rates using conversion factors derived from the nuclear energy releases tabulated by Adamiec and Aitken (1998), to make the results in this work entirely comparable to our other studies on similar deposits and processes in this region (Vandenberghe et al., 2004; 2009; 2013; Kasse et al., 2007; Derese et al., 2009; 2010a, 2010b; 2010c; 2012; Van Mourik et al., 2010; Bogemans and Vandenberghe, 2011). Following Adamiec and Aitken (1998), a reassessment of dose-rate conversion factors has been made by Guérin et al. (2011) and Liritzis et al. (this issue).

A factor of 0.9 (± 5% relative uncertainty) was adopted to correct the external beta dose rates for the effects of attenuation and etching (Mejdahl, 1979). An internal dose rate in quartz grains of 0.013 ± 0.003 Gy ka^{-1} was assumed (Vandenberghe et al., 2008).

The evaluation of the time-averaged moisture content, and the corresponding correction for it of the dose rates, was performed following the procedure outlined in Aitken (1985). The water content in fully saturated samples was measured in the laboratory and ranged in between ~19 % and ~21 %. We adopted a value of 80 ± 20% for the fraction of saturation during burial. Nearness to saturation is expected given the rising sea level since the Late Glacial (e.g. Denys and Baeteman, 1995), the wet maritime climate

system and the general palaeoenvironmental context (wet- and marshlands); the sampled sediments are located near the groundwater table, which is still only at a shallow level below the present topography. A variation of 1% in the time-averaged water content affects the age determination by ~ 1%.

The contribution of cosmic radiation was calculated following Prescott and Hutton (1994), and ranges between ~ 0.15 Gy ka^{-1} and ~ 0.18 Gy ka^{-1}.

Given the dynamic environment, it is difficult to reconstruct former burial history. We used the present day depth and assigned an uncertainty of 15% to these values, which reflects an uncertainty in the burial depth of about 1 m (1 sigma). Cosmic radiation contributes for about 8% to 13% to the total dose rate.

3.6 Optical ages

Table 1 summarises the information relevant to the age and uncertainty calculation. Uncertainties on the luminescence ages were calculated following the error assessment system proposed by Aitken and Alldred (1972) and Aitken (1976). The systematic uncertainty is dominant in the overall uncertainty on the ages and amounts to ~ 8 % (1σ).

As the sources of systematic uncertainty are largely shared between the samples, only the random uncertainty (~ 2 – 6 %) is taken into account to evaluate the internal consistency of the optical ages. Within this uncertainty, the dataset contains no outliers and the age results are consistent with the stratigraphic position of the samples (Table 1; Fig. 6).

Excepting sample GLL-102504, the dates range in between ~ 11 ka and ~ 15 ka. Sample GLL-102504 yields an optical age of 6.8 ± 0.7 ka; the results from small-aliquot analyses (see Section 3.4) suggest that this sample is affected by post-depositional mixing and that the age, therefore, does not accurately reflect the true time of sedimentation.

Nevertheless, it remains clear that the sample consists of initially Late Glacial sediments, as the highest D$_e$s of the distribution correspond to an age of ~11 – 12 ka.

Table 1: Radionuclide activities, estimated time-averaged moisture contents (w.c.), calculated dose rates, equivalent doses (De), optical ages, and random (σr), systematic (σsys) and total (σtot) uncertainties. All uncertainties represent 1σ.

Lab Code (GLL-X)	Depth (m)	Height (m TAW)	^{234}Th (Bq kg^{-1})	^{226}Ra (Bq kg^{-1})	^{210}Pb (Bq kg^{-1})	^{232}Th (Bq kg^{-1})	^{40}K (Bq kg^{-1})	w.c. (%)	Dose rate (Gy ka^{-1})	D_e (Gy)	Age (ka)	σr (%)	σsys (%)	σtot	
														%	ka
102501	3.00	7.14	20 ± 1	23.8 ± 0.4	22 ± 1	27.1 ± 0.3	430 ± 3	16 ± 4	2.10 ± 0.02	25.6 ± 0.6	12.3	2.5	7.8	8.2	1.0
102502	3.15	6.75	19 ± 1	26.1 ± 0.7	26 ± 1	26.7 ± 0.4	420 ± 3	16 ± 4	2.10 ± 0.02	27.7 ± 0.7	13.2	3.2	7.8	8.4	1.1
102503	3.32	6.51	19 ± 1	26.5 ± 0.6	27 ± 1	27.9 ± 0.3	451 ± 4	16 ± 4	2.20 ± 0.02	29.1 ± 1.0	13.2	3.7	7.8	8.6	1.1
102504	2.11	10.84	10 ± 1	10.9 ± 0.8	9 ± 1	10.0 ± 0.3	227 ± 3	15 ± 4	1.21 ± 0.01	8.2 ± 0.4	6.8	6.0	7.5	9.6	0.7
102505	2.37	10.58	9 ± 1	10.1 ± 0.3	10 ± 1	9.1 ± 0.3	273 ± 3	15 ± 4	1.19 ± 0.02	13.6 ± 0.6	11.4	4.4	7.5	8.7	1.0
102506	2.59	10.36	8 ± 1	9.3 ± 0.7	9 ± 1	9.0 ± 0.2	272 ± 3	15 ± 4	1.17 ± 0.01	16.2 ± 0.4	13.9	2.4	7.5	7.9	1.1
102507	2.82	10.23	8 ± 1	8.6 ± 0.2	9 ± 1	9.4 ± 0.2	267 ± 3	15 ± 4	1.15 ± 0.01	17.0 ± 0.6	14.8	3.9	7.5	8.5	1.3
102508	3.04	9.91	8 ± 1	9.0 ± 0.3	8 ± 1	9.1 ± 0.3	288 ± 2	15 ± 4	1.19 ± 0.02	16.8 ± 0.5	14.1	3.2	7.6	8.2	1.2
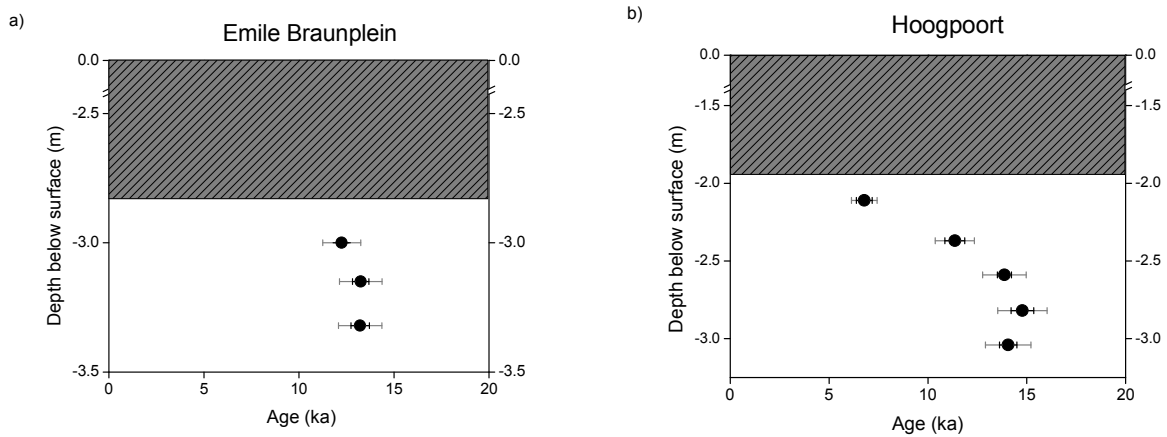
Figure 6: Plot of the optical ages against depth below the surface for (a) the "Emile Braunplein" and (b) the "Hoogpoort". The black and grey error bars represent the random and total uncertainties, respectively.

4. DISCUSSION

Our optical dates of ~11ka - ~15 ka corroborate and refine the Quaternary geological map of the "Zandberg" area, by constraining the chronostratigraphic position of the uppermost aeolian deposits to the Late Glacial. At present, the "Hoogpoort" still represents a small elevation in the historical city centre. The presence of a cart mark in the top of the deposits, in a stratigraphic position below the "black layer", indicates that this relief must have been present at an early stage in the development of the city and has not been changed since then. Historians and city-archaeologists have commonly interpreted any "micro-relief" in the surroundings of the "Blandijnberg" as unimportant or anthropogenic, i.e. either as figments of imagination or as man-made mounds; our results provide firm evidence of the contrary.

At many localities in East Flanders, and in urban environments in particular, much of the original topography has been artificially levelled. In and near the city of Ghent, mining of wind-blown sands (Heins, 1923) and infrastructural works (such as road construction; Dumont, 1951) are likely to have removed the top of the sequences, and thus the most recent part of the sedimentary record. Consequently, it remains a challenge to establish when sedimentation ended. Also, the start of sedimentation could not be documented, as the base could not be sampled.

Although the two sequences are composed of sediments of more or less the same age, we observed significant granulometric differences be-

tween the two sequences. A more detailed grain size determination might provide more information on the exact depositional mechanisms.

At present, the sedimentary archive in Ghent is scarce and extremely difficult to access (heavily asphalted and built on). Considering this difficulty in obtaining physical evidence, historical landscape depictions, maps and toponyms may signify a unique tool to reconstruct the past environmental setting of Ghent.

5. CONCLUSIONS

We distance ourselves from the idea that the "Blandijnberg" was the main environmental factor governing the setting, development, subsis-tence and general functioning of the city of Ghent. The subsurface of the historical centre of Ghent consists of Late-Pleniglacial / Late Glacial aeolian sands. It follows that this sandy environment, including its microrelief and hydrological network, should be considered when trying to understand Ghent in its environmental context.

Our exploratory study confirms the value of historical depictions, cartographic maps and toponyms to reconstruct the palaeo-microrelief. Understanding these deposits in terms of climate or anthropogenic forcing, however, remains a challenge as the sequences have been largely obliterated by anthropogenic intervention.

REFERENCES

Adamiec, G., Aitken, M. (1998) Dose-rate conversion factors: update. *Ancient TL*, vol. 16, 37-50.

Aitken, M.J. (1976) Thermoluminescence age evaluation and assessment of error limits: revised system. *Archaeometry*, vol. 18, 233-238.

Aitken, M.J. (1985) *Thermoluminescence dating*. Academic Press Inc., London. 359 pp.

Aitken, M.J., Allred, J.C. (1972) The assessment of error limits in thermoluminescence dating. *Archaeometry*, vol. 14, 257-267.

Bogemans, F., Vandenberghe, D. (2011) OSL dating of an inland dune along the lower River Scheldt near Aard (East Flanders, Belgium). *Netherlands Journal of Geosciences,* vol. 90, 23-29.

Bøtter-Jensen, L., Andersen, C.E., Duller, G.A.T., Murray, A.S. (2003) Developments in radiation, stimulation and observation facilities in luminescence measurements. *Radiation Measurements*, vol. 37, 535-541.

Capiteyn A., Charles L., Laleman M.C. (2007) *Historische Atlas van Gent*. SUN Amsterdam, 80 pp.

Castel, I., Koster, E., Slotboom, R. (1989) Morphogenic aspects and age of Late Holocene eolian drift-sands in Northwest Europe. *Zietschrift für Geomorphologie*, vol. 33, 1-26.

Cunningham, A.C., Wallinga, J. (2010) Selection of integration time intervals for quartz OSL decay curves. *Quaternary Geochronology*, vol. 5, 657-666.

De Corte, F., Vandenberghe, D., De Wispelaere, A., Buylaert, J-P., Van den haute, P. (2006) Radon loss from encapsuled sediments in Ge gamma-ray spectrometry for the annual radiation dose determination in luminescence dating. *Czech Journal of Physics*, vol. 56, D183-D194.

De Moor, G. (1981) Periglacial deposits and sedimentary structures in the upper Pleistocene infilling of the Flemish Valley (NW Belgium). *Biuletyn Peryglacjalny*, vol. 28, 277-291.

Denys, L., Baeteman, C. (1995) Holocene evolution of relative sea-level and local mean high water spring tides in Belgium: a first assessment. *Marine Geology*, vol. 124, 1-19.

Derese, C., Vandenberghe, D., Eggermont, N., Bastiaens, J., Annaert, R., Van den haute, P. (2010a). A medieval settlement caught in the sand: optical dating of sand drifting at Pulle (N-Belgium). *Quaternary Geochronology*, vol. 5, 336-341.

Derese, C., Vandenberghe, D., Paulissen, E., Van den haute, P. (2009) Revisiting a type locality for Late Glacial aeolian sand deposition in NW Europe: Optical dating of the dune complex at Opgrimbie (NE Belgium). *Geomorphology*, vol. 109, 27-35.

Derese, C., Vandenberghe, D., van Gils, M., Mees, F., Paulissen, E., Van den haute, P. (2012) Final Palaeolithic settlements of the Campine region (NE Belgium) in their environmental context: Optical age constraints. *Quaternary International*, vol. 251, 7-21.

Derese, C., Vandenberghe, D., van Gils, M., Vanmontfort, B., Meirsman, E., Mees, F., Van den haute, P. (2010c) Establishing a chronology for landscape evolution around a final paleolithic site at Arendonk-Korhaan (NE Belgium): First results from OSL dating. *Mediterranean Archaeology and Archaeometry*, vol. 10(4), 43-51.

Derese, C., Vandenberghe, D.A.G., Zwertvaegher, A., Court-Picon, M., Crombé, P., Verniers, J., Van den haute P. (2010b) The timing of aeolian events near archaeological settlements around Heidebos (Moervaart area, N Belgium). *Netherlands Journal of Geosciences*, vol. 89, 173- 186.

Duller, G.A.T. (2003) Distinguishing quartz and feldspar in single grain luminescence measurements; *Radiation Measurements*, vol. 37, 161-165.

Dumont, M. (1951) *Gent, een stedenaardrijkskundige geschiedenis*. Brugge, De Tempel. 590 pp.

Fuchs, M., Lang, A. (2009) Luminescence datings of hillslope deposits - A review. *Geomorphology*, vol. 109, 17-26.

Gelaude, F. (2010a) Rivierduinen en dekzanden. *Erfgoedmemo GVSA*, 44.

Gelaude, F. (2010b) Waterbeheer in een middeleeuwse grootstad: stuwen en dammen te Gent (12-14de eeuw). *Jaarboek voor Ecologische Geschiedenis*, Gent Academia Press, p33-53.

Guérin, G., Mercier, N., Adamiec, G. (2011) Dose-rate conversion factors: update. *Ancient TL*, vol. 29(1), 5-8.

Gysseling, M.E. (1954) *Gent's vroegste geschiedenis in de spiegel van zijn plaatsnamen*. Antwerpen. Standaard, 87 pp.

Heins, M. (1923) *Gand, sa vie et ses institutions*. Deel 2. Gent, Maison d'Editions et d'Impressions Anciennement Ad. Hoste, 704 pp.

Kasse, C. (1999) Late Pleniglacial and Late Glacial aeolian phases in The Netherlands. In: W. Schirmer (ed.) *Dunes and fossil soils. GeoArchaeoRhein*, vol. 3, 61-82.

Kasse, C. (2002) Sandy aeolian deposits and environments and their relation to climate during the Last Glacial Maximum and Lateglacial in northwest and Central Europe. *Progress in Physical Geography*, vol. 26, 507–532.

Kasse, C., Vandenberghe, D., De Corte, F., Van den haute, P. (2007) Late Weichselian fluvio-aeolian sands and coversands of the type locality Grubbenvorst (southern Netherlands): sedimentary environments, climate record and age. *Journal of Quaternary Science*, vol. 22(7), 695-708.

Koster, E.A. (1988) Ancient and modern cold-climate aeolian sand deposition: a review. *Journal of Quaternary Science*, vol. 3, 69-83.

Liritzis, I., Stamoulis, K, Papachristodoulou, C, and Ioannides, K (2013) A re-evaluation of radiation dose-rate conversion factors. *Mediterranean Archaeology & Archaeometry*, vol. 13(3), 1-15.

Mejdahl, V. (1979) Thermoluminescence dating: beta-dose attenuation in quartz grains. *Archaeometry*, vol. 21, 61-72.

Murray, A.S., Wintle, A.G. (2003) The single aliquot regenerative dose protocol: potential for improvements in reliability. *Radiation Measurements*, vol. 37, 337-381.

Prescott, J.R., Hutton, J.T. (1994) Cosmic ray distributions to dose rates for luminescence and ESR dating: large depths and long-term time variations. *Radiation Measurements*, vol. 23, 497-500.

Tavernier, R. (1936) Bijdrage tot de geologie van de stad Gent. *Natuurwetenschappelijk tijdschrift*, vol. 29(4), 149-166.

Tavernier, R. (1954) Le Quaternaire. *Prodrome d'une description Géologique de la Belgique (Liège)*, Luik, 565-589.

van Mourik, J.M., Nierop, K.G.J., Vandenberghe, D. (2010) Radiocarbon and optically stimulated luminescence dating based chronology of a polycyclic drift sand sequence at Weerterbergen (SE Netherlands). *Catena*, vol. 80, 170-181.

Vandenberghe, D. (2004) *Investigation of the optically stimulated luminescence dating method for application to young geological samples*. Ph.D. Thesis, Universiteit Gent.

Vandenberghe, D., De Corte, F., Buylaert, J-P., Kučera, J., Van den haute, P. (2008) On the internal radioactivity in quartz. *Radiation Measurements*, vol. 43, 771-775.

Vandenberghe, D., Derese, C., Kasse, C., Van den haute, P. (2013) Late Weichselian (fluvio-)aeolian sediments and Holocene drift-sands of the classic type locality in Twente (E Netherlands): a high-resolution dating study using optically stimulated luminescence. *Quaternary Science Reviews*, vol. 68, 96-113.

Vandenberghe, D., Kasse, C., Hossain, S.M., De Corte, F., Van den haute, P., Fuchs, M., Murray, A.S. (2004b) Exploring the method of optical dating and comparison of optical and ^{14}C ages of Late Weichselian coversands in the southern Netherlands. *Journal of Quaternary Science*, vol. 19(1), 73-86.

Vandenberghe, D., Vanneste, K., Verbeeck, K., Paulissen, E., Buylaert, J-P., De Corte, F., Van den haute P. (2009) Late Weichselian and Holocene earthquake events along the Geleen fault in NE Belgium: OSL age constraints. *Quaternary International*, vol. 199, 56–74.

Verbruggen, C., Denys, L., Kiden, P. (1991) Paleo-ecologische en geomorfologische studie van Laag- en Midden-België tijdens het Laat-Kwartair. *De Aardrijkskunde*, vol. 3, 357-376.

Vermeire, S., De Moor, G., Adams, R. (1999) *Quartairgeologische Kaart van België, Vlaams Gewest, Verklarende tekst bij het Kaartblad (22) Gent (1/50.000)*. Haecon n.v, rapport, Afdeling Natuurlijke Rijkdommen en Energie, Brussel. 68 pp.